Report of the experiment SI-2345 performed at BM08 "GILDA" beamline

October 26th – November 1st, 2011

Team

Maurizio Romanelli – Univ. Florence (Italy)

Francesco Di Benedetto, *principal investigator* – Univ. Florence (Italy) - francesco.dibenedetto@unifi.it

Ilaria Bencistà – Univ. Florence (Italy)

Silvia Frizzera – Univ. Florence (Italy)

Giordano Montegrossi – CNR-IGG, Florence (Italy)

Francesco D'Acapito, *local contact* – CNR-IOM, OGG c/o ESRF, Grenoble (France)

Premise

The beamtime was divided approximately in two equivalent parts, dedicated at measurements at the Sn and Cu K edge respectively. At both edges, two kind of samples were investigated (together with the relevant standards): nanopowders of ternary and quaternary kesterite-like materials, and solar cells containing thin films of binary ternary and quaternary sulfides, still belonging to the same kesterite-stannite-kuramite system. Owing to the fact that the investigated samples are largely different, implying different experimental approaches, the correpsonding results are exposed separately in the following paragraphs.

1 – nanopowders

1.1 – Experimental procedures

All measurements were carried out at the Beamline BM08 at the ESRF. The list of the investigated samples is reported in Table 1. Samples st1495 and st1499/51 are natural specimens belonging to the Natural History Museum of Florence, and represent the most studied stannite reference materials (something like "international standards"). Stsyn is a synthetic sample obtained by a conventional synthetic route. St1495, st1499/51 and stsyn are indistinguishable by XRD, i.e. they are supposed to have exactly the same structure. NkurM and nst2 are two synthetic samples obtained through a novel solvothermal route. From XRD inspection, they seem to have the same structural model as that of standards, but with random cation distribution.

Table 1

sample	Chemical formula	Structural reference	Sn K edge spectrum	Cu K edge spectrum	Type
St1495	$Cu_{1.97}Fe_{0.92}Zn_{0.07}Sn_{1.01}S_{4.03}$	Bonazzi	Transmission	Transmission	Std
St1499/51	$Cu_{2.04}Fe_{0.78}Zn_{0.24}Sn_{1.01}S_{3.94}$	Bonazzi	Transmission	Transmission	Std
Stsyn	Cu_2FeSnS_4	Bonazzi	Transmission	Transmission	Std
nkurM	Cu_3SnS_4	unknown	Transmission	Transmission	Unk
nst2	$Cu_{2.9}Fe_{0.1}SnS_4$	unknown	Transmission	Transmission	Unk

All spectra were registered under vacuum at 80 K, in the Transmission mode, both at the Cu and Sn K- edges (8979 and 29200 eV, respectively). In addition to the samples of Table 1, most of the main sulphide minerals relevant to this investigation were analysed: CuS, covellite, Cu_2S, chalcocite, $CuFeS_2$, chalcopyrite, Cu_5FeS_4, bornite, Cu_3AsS_4, enargite; SnS, herzenbergite. Also non-sulfide minerals were investigated at the Sn K-edge: SnO, SnO_2, $SnCl_2.2H_2O$, $SnSO_4$.

EXAFS data were extracted from the raw absorption coefficient spectrum with the ATHENA code. Data were analysed in the k-range, k = [2.8–12.0] $Å^{-1}$, and were Fourier transformed in the R interval, R = [0.8–6] Å.

1.2 – Results

In general, at both Cu and Sn K edges, the three stannite samples exhibit spectra adequately close to those of the unknown samples. As a consequence, we are confident that these three standards represent a good reference for the interpretation of the EXAFS data of our sulfides. In the following we will focus our comparison only to these references.

Sn K edge

The edge positions observed for the five considered samples are summarised in Table 2. There are significant shifts of the edge position, in particular with respect to the smallness of the changes in the chemical composition.

Table 2

sample	Edge position (Sn)	Edge position (Cu)
St1495	29221.5	8982.5
St1499/51	29220.1	8981.6
Stsyn	29220.6	8982.9
nkurM	29222.0	8982.1
nst2	29221.0	8982.6

The $\chi(k)$ data for the natural samples (st1495 and st1499/51) present a clear evidence of a contribution from successive shells. The same holds true for the stsyn sample. On the contrary, the EXAFS extracted from the unknown samples are

definitely simpler. At a first insight, only a single shell can be clearly revealed. A Figure comprehensive of all $\chi(k)$ data is shown (Fig. 1).

Starting from these consideration, we proceeded with the Fourier Transforms in the R-range from 2.8 to 10/12 (depending on the spectral noise at the high k values). A comparison of the resulting spectra in the R space, shown in the Figure 2, allows to infer that:

1) the first shell of nst2 appears split in two components.

2) the first shell of the samples nkurM, nst2 and st1495 occurs at the same position; on the contrary, for st1499/51 it occurs at a lower distance and for stsyn it occurs at a higher distance.

3) samples st1495 and st1499/51 exhibit a clear fingerprint of a split second shell; the same features are present in the spectrum of stsyn with lower intensity, whereas in the nst2 and nkurM spectra they are almost masked by the FT noise.

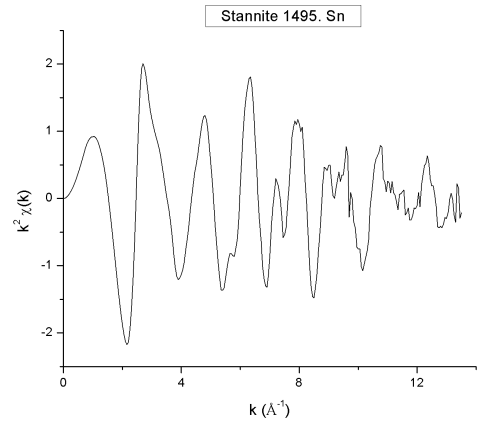

a

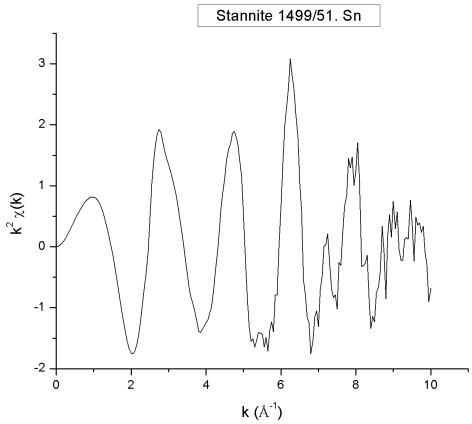

b

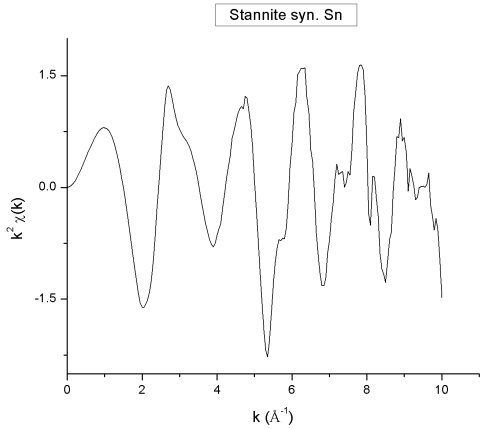

c

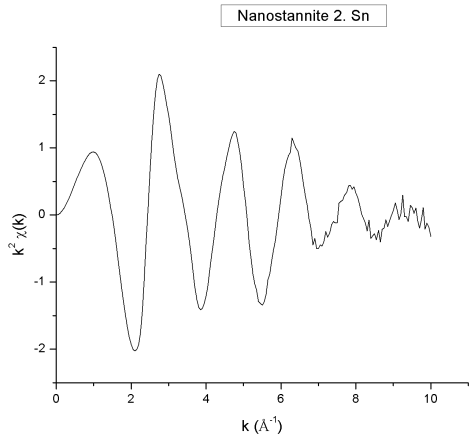

d

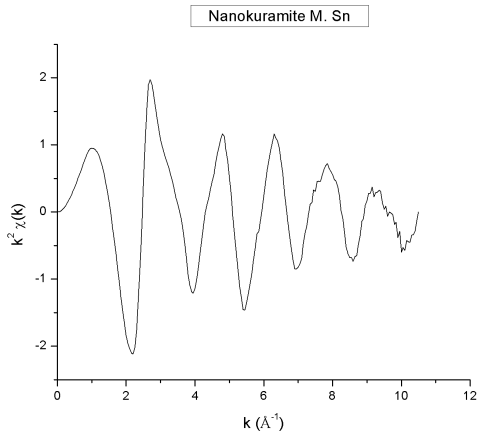

e

Figure 1 – EXAFS at the Sn K edge of stannites (a–c) and nanopowders (d–e)

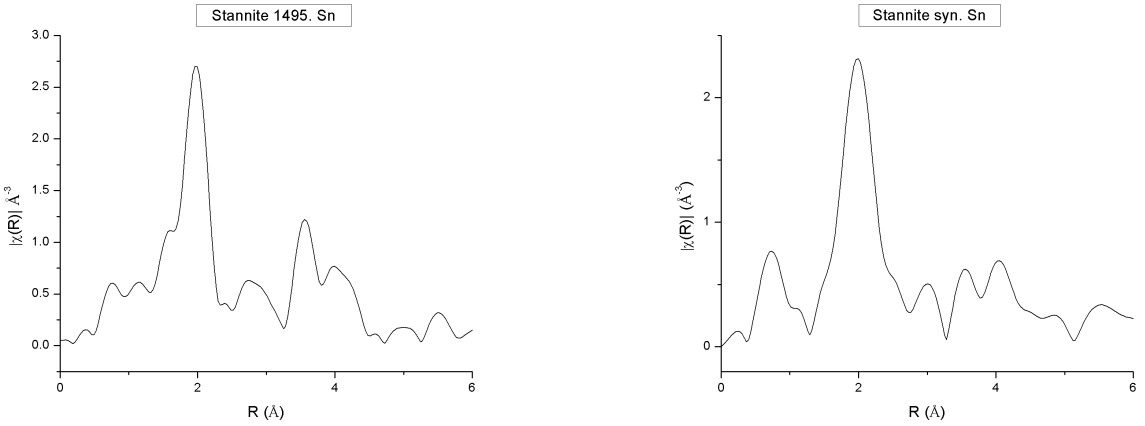

a

b

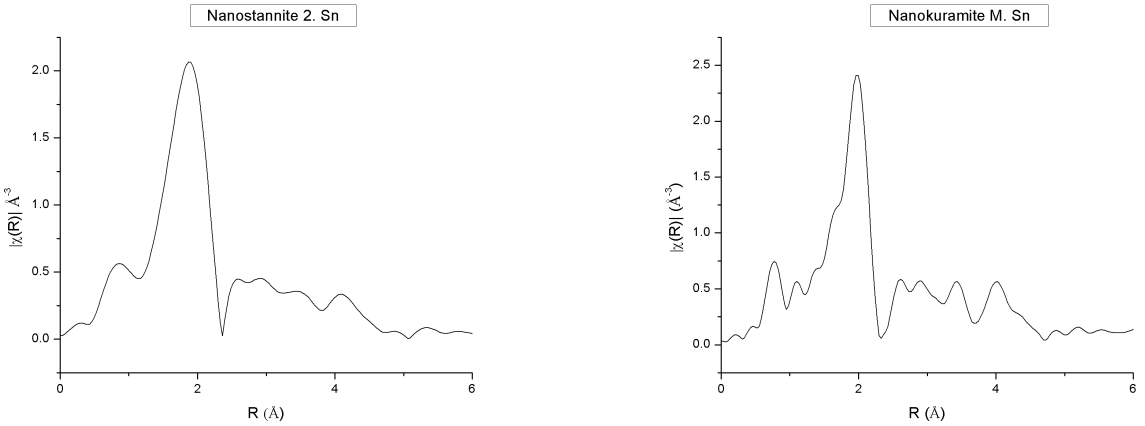

c

d

Figure 2 – FTs of the EXAFS at the Sn K edge of stannites (a–b) and nanopowders (d–e)

Cu K edge

The χ(k) data for the natural and synthetic standards (st1495, st1499/51 and stsyn) present a clear evidence of a contribution from successive shells. On the contrary, the EXAFS extracted from the unknown nst2 sample is definitely simpler. At a first insight, only a single shell can be clearly revealed. The nkurM spectrum reveals an intermediate case: fingerprints of successive shell contributions are apparent. A Figure comprehensive of all χ(k) data is shown below (Fig. 3).

We proceeded with the Fourier Transforms in the R-range from 2.8 to 10/12 (depending on the spectral noise at the high k values). A comparison of the resulting spectra in the R space (Fig. 4) allows to infer that:

1) samples st1495, st1499/51 and stsyn exhibit a clear fingerprint of a split second shell;

2) an almost negligible evidence of a second shell is observed for nst2

3) sample nkurM reveals a split second shell signal occurring at exactly the same R values of those of the natural samples, but exhibiting a more complex structure.

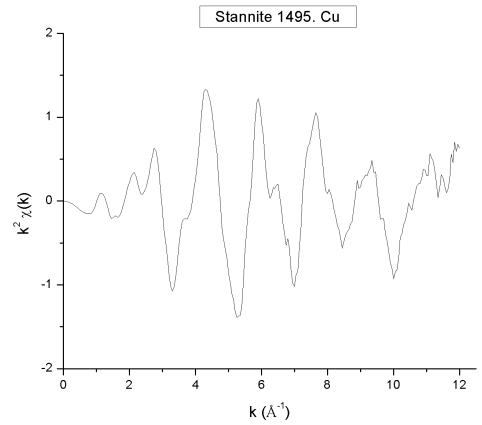

a

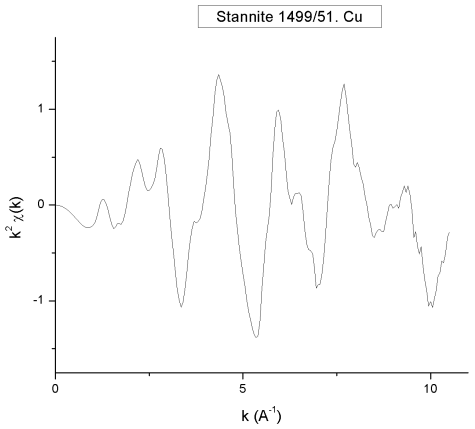

b

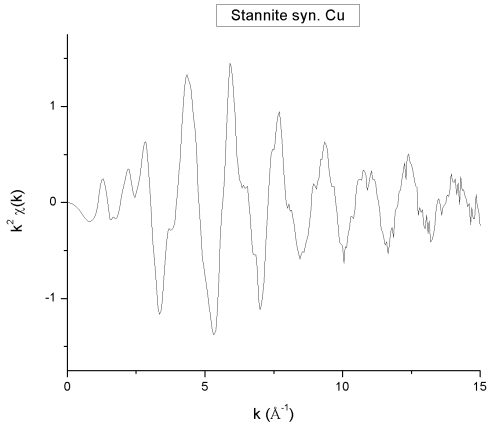

c

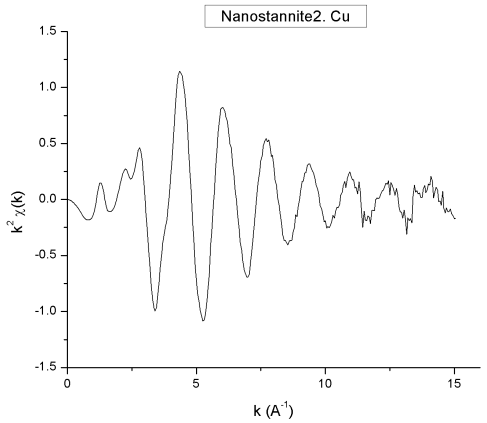

d

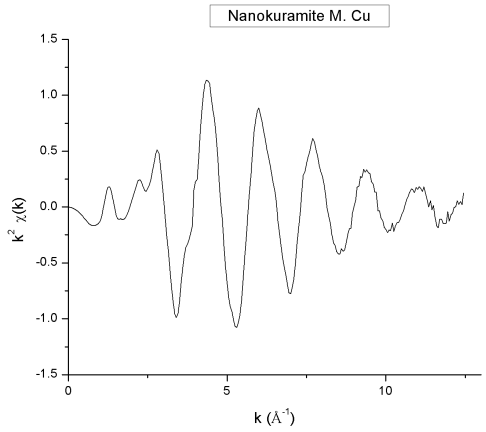

e

Figure 3 – EXAFS at the Cu K edge of stannites (a–c) and nanopowders (d–e)

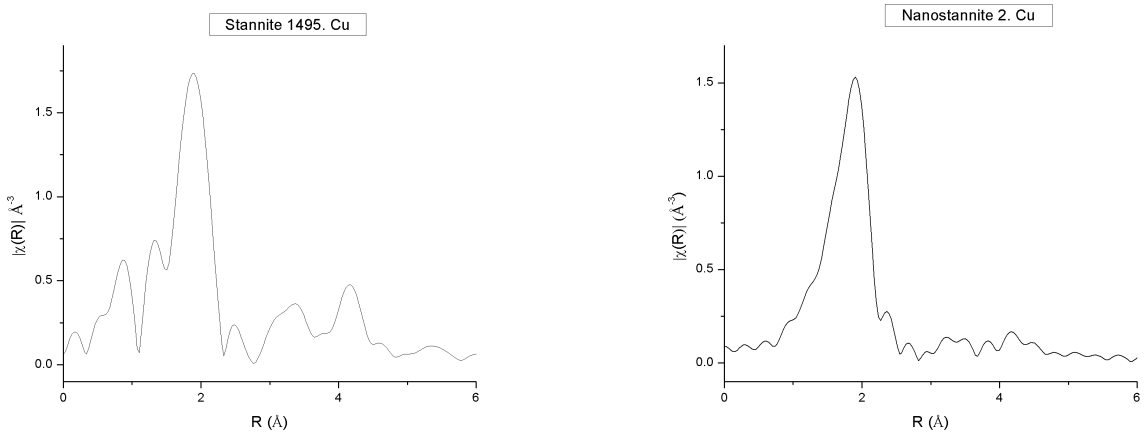

a b

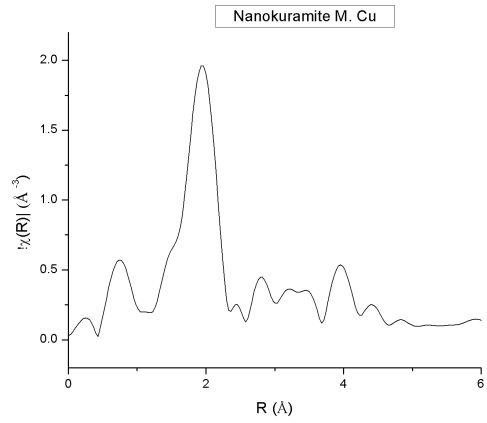

c

Figure 4– FTs of the EXAFS at the Cu K edge of stannite (a) and nanopowders (b–c)

2 – Thin films of binary, ternary and quaternary compounds deposited on Ag(111)

2.2 – Experimental procedure

The samples consist of thin films of binary, ternary and quaternary sulphides of CuS, $Cu_xSn_yS_z$, and $Cu_xSn_yZn_wS_z$ deposited by ECALD (ElectroChemical Atomic Layer Deposition) onto a single crystal of Ag(111). This technique allows to obtain a layer-by-layer growth of these compounds, based on a particular phenomena of surface limited deposition of the elements, namely UPD (Underpotential Deposition) [1]. Every samples is realized performing n cycles of deposition of a chosen sequence. The samples investigated are summarized in Table 4. Three different samples of ternary compound were prepared changing the stoichiometric ratio between the number of layers of Cu and Sn.

Table 4

Sample name	Chemical formula	Sequence of deposition	Number of cycles (n)	label
Bin	CuS	$Ag/S/(Cu/S)_n$	20	binCuS20A5
Ter1	$Cu_xSn_yS_z$	$Ag/S/(Cu/S/Sn/S)_n$	10	ter117G
Ter2	$Cu_xSn_yS_z$	$Ag/S/(Cu/S/Cu/S/Sn/S)_n$	7	ter21H
Ter3	$Cu_xSn_yS_z$	$Ag/S/(Cu/S/Sn/S/Sn/S)_n$	7	ter127E
Quat	$Cu_xSn_yZn_wS_z$	$Ag/S/(Cu/S/Sn/S/Zn/S)_n$	7	quat1117L

The XAS spectra were acquired in the Fluorescence mode, having put the Ag electrode in the Grazing incidence position. In this way, the synchrotron radiation is only partly incident on the film. Acquisition times were significantly long, in order to improve the Intensity-to-noise ratio. Spectra were registered at both the Cu and Sn K edges, but in this case, the experiment were unsuccesful, due to the overlap of a Silver fluorescence spectrum in the energy region of the Sn K edge. Instead, at the Cu K edge, the spectra were acquired with conceivable easyness, although the total counts were low. Thus, most of the experimental beamtime was dedicated to the acquisition of multiple scans over the set of available films (Table 4).

Results

The registered spectra in the pre-edge and XANES region are shown in Figure 6. The spectra are apparently different for both edge position and XANES features: e.g., only two samples exhibit a "white line" unsual for tetrahedral Cu in sulfide). We decided to compare these two samples, ... and ..., with some oxidised standard, to verify if some

oxidation has occurred in the sample (before or during the sample preparation and the measurements). The Figure 7 evidence that only a partial similarity can be fostered between the spectra of the films and those of Cu(II) oxide and Cu carbonate (malachite). Accordingly, if present only a partial oxidation can be suggested from these data. Nevertheless, as evident in Figure 6, the resemblance of these features with those of bulk stannite-like materials is very poor.

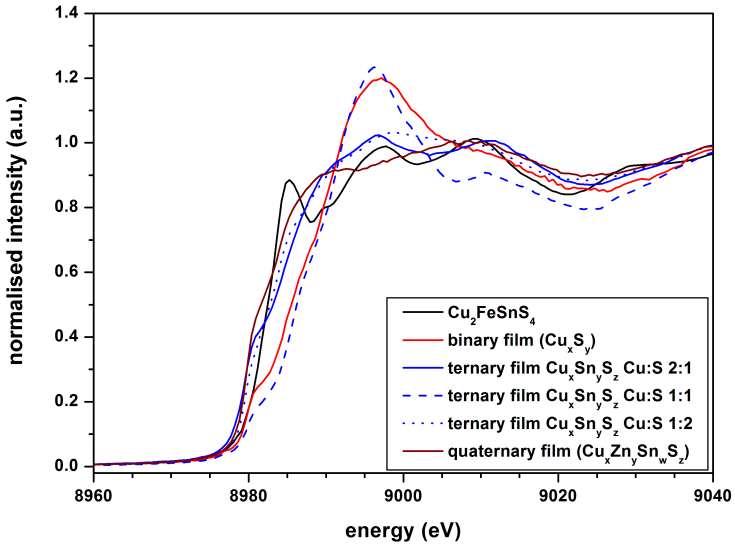

Figure 6 – pre-edge and XANES region of thin films, compared with those of stannite

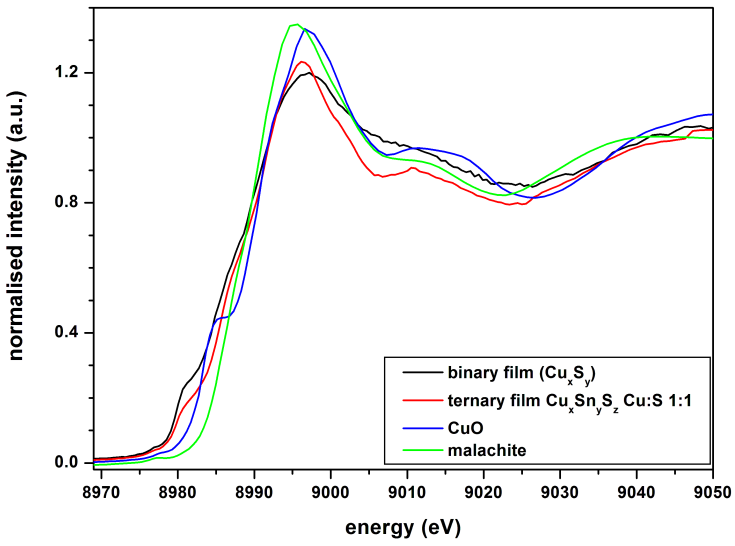

Figure 7 – pre-edge and XANES region of selected thin films, compared with those of some oxidised Cu samples

The EXAFS spectra of the thin films are obviously noisy, and only a limited k-range can be useful for the structural investigation (Figg. 8a-8c). Nevertheless, it is apparent a significant change in the period of the EXAFS, that implies significant differences at least in the distance of the first coordination shell.

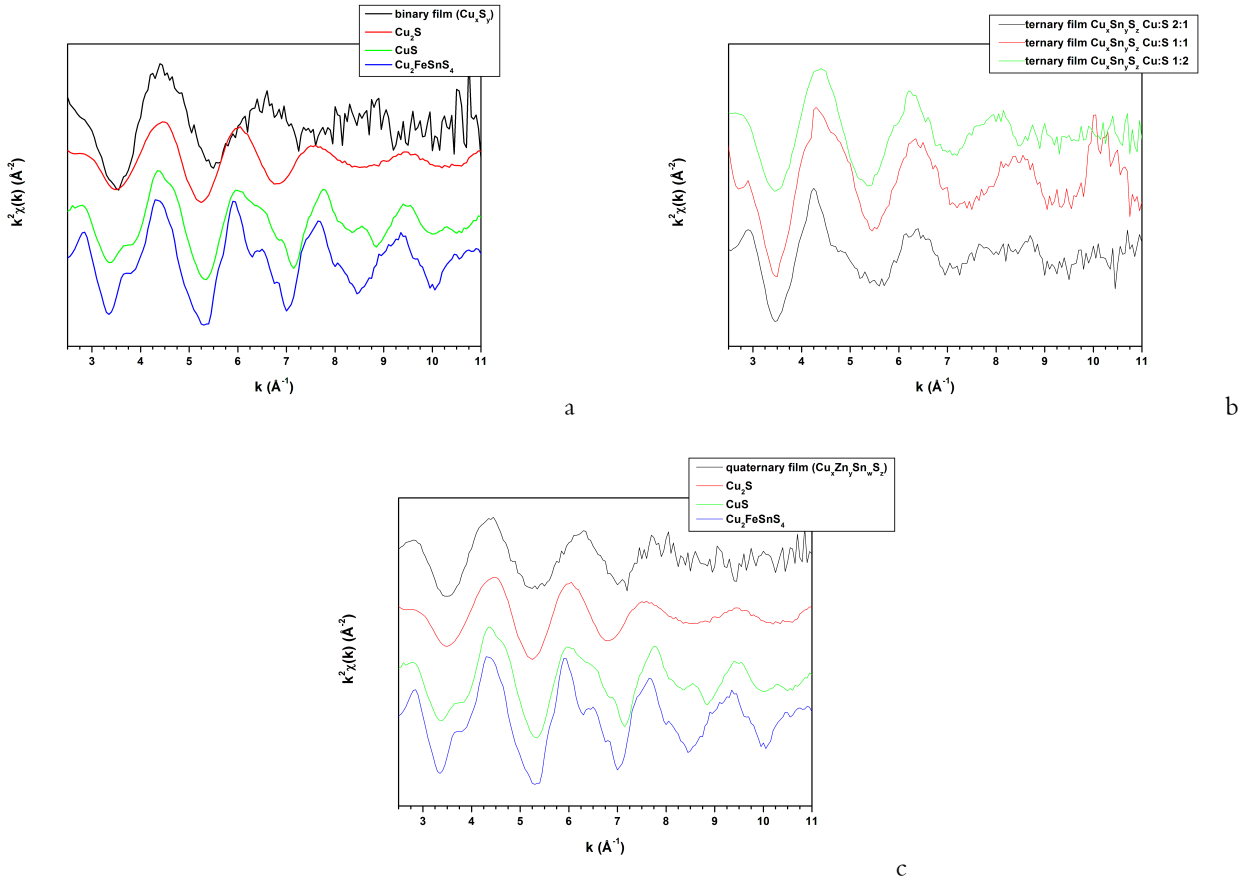

Figure 8 – EXAFSs registered in the thin films: a) binary film, b) ternary films, c) quaternary film. The binary and quaternary films are compared with those of some pertinent sulfide standards.

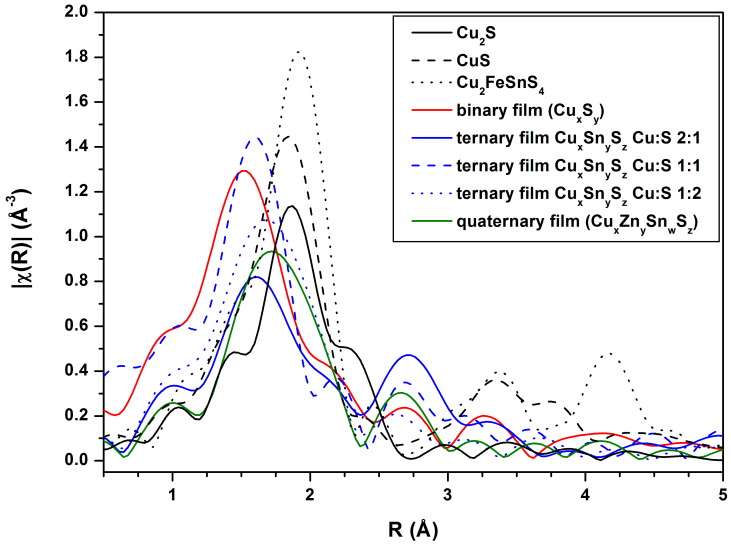

Figure 9 – FT of the epxerimental EXAFSs of thin films, compared with those of some pertinent sulfide standards.

Moreover, less marked but still appreciable differences can be devised in the EXAFSs of the different films. Accordingly, when Fourier Transformed in the R space, the first shell peak presents a consistent variability among the considered samples (Figure 9).

The peculiar spectral features revealed by the investigated films are of difficult interpretation. An attempt of simply attributing the differences from the sulfide standards to oxidation of the Cu was pursued, by a preliminary fit. However, this fit should exclude a relevant role played by oxidation (D'Acapito, personal communication).

Accordingly, we are able to highlight some considerations:

1) thin films are structurally different from the quaternary chalcogenides (either bulk or nanocrystalline). This is mainly due to the fact that Cu-S distances are significantly shorter.

2) although a precise attribution of the valence states is not yet available (spectra are under interpretation), it appears likely that Cu is mainly monovalent

3) only a partialy oxidation of the film could be considered: if present, this phenomenon appears not ubiquitous nor prevailing